Pol. J. Environ. Stud. Vol. 32, No. 1 (2023), 965-972
DOI: *10.15244/pjoes/155094* ONLINE PUBLICATION DATE: 2022-12-05

Short Communication

Enhanced Nitrogen Removal Performance in Constructed Wetland by Coupling Partial Tide Flow Operation Mode with Iron-Carbon Micro-Electrolysis Process

Yi Ding[1,2], Yitong Ji[1], Yuan Sun[1], Xinshan Song[2], Ran Ding[1], Liwen Zhang[1], Xuan Yang[1], Xingpo Liu[1]*

[1]College of Ocean Science and Engineering, Center for Marine Environmental and Ecological Modelling, Shanghai Maritime University, Shanghai 201306, China
[2]College of Environmental Science and Engineering, State Environmental Protection Engineering Center for Pollution Treatment and Control in Textile Industry, Donghua University, Shanghai 201620, China

Received: 4 June 2022
Accepted: 2 October 2022

Abstract

Constructed wetlands (CWs) with iron-carbon (Fe-C) filler and gravel filler were set up to examine the synthetic effects of partial tide flow operation mode and Fe-C micro-electrolysis on nitrogen removal performance. Submerged emptying ratio (SER) that representing flood and drain period was set to 2:1 and 1:2 respectively for creating aerobic/anoxic alternative conditions. Upper nitrification area of CWs was operated by tide flow mode and the transformation of NH_4^+-N to NO_3^--N was greatly enhanced via the extension of emptying time for air dissolution. Fe-C micro-electrolysis could enhance the availability of carbon sources for biological denitrification and facilitated autotrophic denitrification based on iron oxidation and transfer. It made clear that enhanced denitrification in bottom area contributed to NO_3^--N removal from water body thus facilitating TN removal. Comprehensive and stable COD (84.2±2.0%), NO_3^--N (82.1±2.0%) and TN (55.6±2.0%) removal efficiencies were simultaneously achieved in partial tide flow CW with Fe-C filler under SER of 1:2. The study provided a novel idea for the efficient nitrogen removal in CWs treating eutrophic water.

Keywords: constructed wetland, nitrogen removal, iron-carbon micro-electrolysis, partial tide flow operation mode, submerged emptying ratio

*e-mail: xpliu@shmtu.edu.cn

Introduction

With the rapid development of economy and human activities, nitrogen emission and pollution into freshwater has seriously affected human health and water quality safety [1]. Excessive nitrogen is even a major factor leading to eutrophication of waterbodies [2]. Constructed wetland (CW) is a low-cost and highly effective water treatment technology, which has been widely used in nitrogen removal of various wastewater [3]. Microbial nitrification and denitrification is the main nitrogen removal mechanism in CWs [4]. Aerobic condition usually benefits nitrification but limits the denitrification process. Hence, rational control of oxygen distribution and content was crucial for creating alternant aerobic and anoxic conditions for nitrification and denitrification [5]. Additionally, denitrification process is mainly influenced by inadequate carbon sources [6]. The depletion of oxygen and electron donor due to wetland configuration and low C/N characteristic of wastewater led to incomplete total nitrogen (TN) removal efficiency in traditional CWs [7]. Although external carbon addition and artificial aeration strategies have been proven effective in supplementing carbon sources and oxygen, both strategies are high-cost and unsuitable for long-term utilization [8]. It is imperative to develop an economic strategy to promote CW performance for permanent applications. Optimization of wetland configuration and operation mode would be conducive to promote nitrogen transformation and removal economically and efficiently [9]. Tidal flow CW creates rhythmic cycles of filled and drained status of the wetland matrix, which promotes the dissolution of atmospheric air into CW bed [10]. The operational strategy for CW reoxygenation is relatively low-cost and suitable for long use. Submerged emptying ratio (SER) represents different flood and drain periods, which plays a key role in determining aerobic/anoxic condition and affecting oxidation-reduction potential for nitrogen transformation and removal [11]. Nevertheless, most researchers focused primarily on filled and drained phase of the whole area in tidal flow CWs, which may not provide significantly altering aerobic/anoxic conditions for the simultaneous occurrence of nitrification and denitrification. Denitrification would be inhibited by high oxygen content or carbon deficiency thus affecting TN removal [12]. Adopting tidal flow operation mode in part area of CW is expected to provide differential oxygen environment for efficient nitrogen removal. Iron-carbon (Fe-C) micro-electrolysis technology transforms the macro-molecular refractory organics into the micro-molecular biodegradable organics, which could enhance the available carbon and generates hydrogen and Fe^{2+} as electron donor [13]. Hence, it is of great significance to combine iron and carbon materials in CWs, which is expected to solve the problem of insufficient carbon source by achieving facultative autotrophic heterotrophic denitrification [14]. However, little research is known about the synthetic effects of partial tide flow operation mode and iron-carbon micro-electrolysis on nitrogen removal performance of CW.

In this study, tidal flow operation mode was adopted in upper nitrification area of CW, and the effect of submerged emptying ratio on reoxygenation and nitrogen transformation was described and analyzed. Additionally, Fe-C filler was put on the upper nitrification area and bottom denitrification area of CW respectively to investigate micro-electrolysis effect on nitrogen removal. Synergistic effect of partial tide flow operation mode and iron-carbon micro-electrolysis process on nitrification and denitrification performance was evaluated. The study aimed to provide the accurate

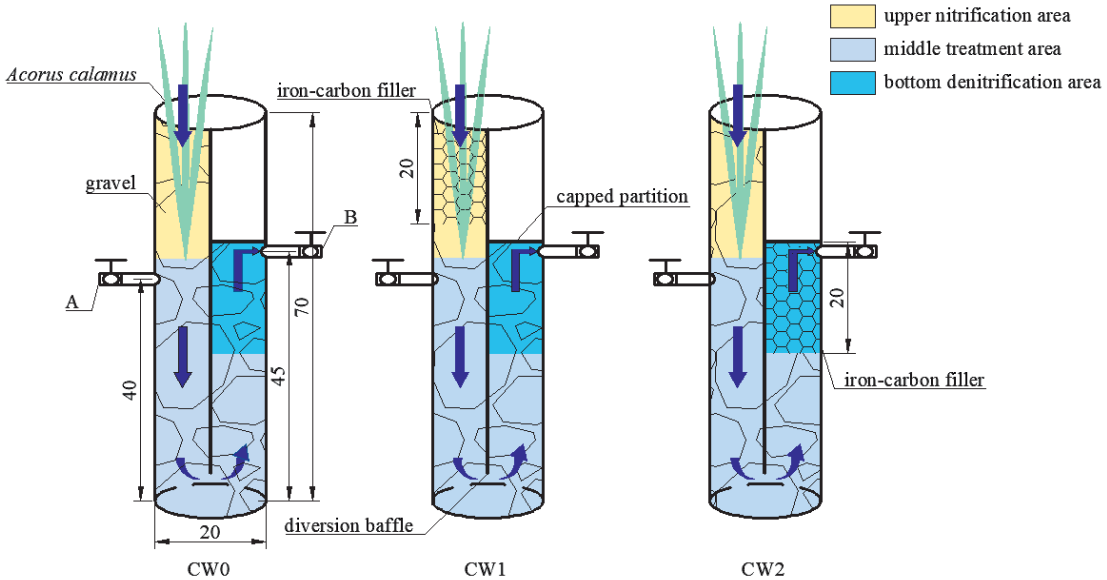

Fig. 1. Schematic diagram of the experimental CWs.

understanding of nitrogen removal mechanisms in partial tide flow CW coupled with Fe-C micro-electrolysis for advanced water purification.

Material and Methods

Three lab-scale CW microcosms were constructed by organic glass columns with inner diameters of 20 cm and heights of 70 cm. The schematic diagram of experimental systems is shown in Fig. 1. A 65-cm division baffle was placed in the middle of CWs with the depth of 5 cm from the bottom while a capped partition was placed in the right side of division baffle with the depth of 45 cm from the bottom. Each microcosm was separated by division baffle and divided into three areas: (1) upper nitrification area; (2) middle treatment area; (3) bottom denitrification area. Upper nitrification area was operated by tidal flow mode while bottom denitrification area served as the drainage layer. Two sampling points were located at the outlet section of upper nitrification area and bottom denitrification area with the depth of 40 cm (A) and 45 cm (B) from the bottom. CW0 was blank group and packed with 3-4 cm sizes gravel. Upper nitrification area of CW1 was packed with 3-4 cm sizes Fe-C filler while other areas of CW1 were filled with 3-4 cm sizes gravel. Correspondingly, bottom denitrification area of CW2 was packed with 3-4 cm sizes Fe-C filler while other areas of CW2 were filled with 3-4 cm sizes gravel. The main raw materials of Fe-C filler were iron powder, activated carbon, bentonite and metal catalyst. Iron powder and activated carbon were mixed with the mass ratio m (Fe): m (c) = 3:1. Bentonite and metal catalyst were added accounting for 10% and 5% respectively in the total mass of Fe-C filler. Raw materials were sintered at high temperature for forming spherical and porous particles. The microcosms were planted with four stems of *Acorus calamus* with similar height and growth statuses. Synthetic wastewater was used in this study and the influent characteristics were reflected in Table 2.

The experiments were divided into two phases and each phase was 7 days. The CWs created flood and drain cycle via peristaltic pumps controlled by pre-programmed timer. Each cycle was rhythmically repeated every 24 h at room temperature. The substrate of upper nitrification area would be periodically exposed in air after wastewater within the area was discharged or periodically submerged in water along with the variation of SER (named partial tide flow operation area), while the substrate within other areas would be invariably submerged in water. At the first phase, SER was set to 2:1 that providing 16 hours of anaerobic during the flood status and 8 hours oxygenation during the emptying status. At the second phase, SER was set to 1:2 that providing 8 hours of anaerobic during the flood status and 16 hours oxygenation during the emptying status. During the drainage stage of each cycle, wastewater in the upper nitrification area was discharged through the sampling port B and stored in effluent tanks, which would be fed back into upper nitrification area next day, thus enhancing oxygen dissolution and diffusion. Samples were collected each day for analysis of physical and chemical indexes. The pH value was determined immediately using a pH meter (PH-838, SMART SENSOR, China). Dissolved oxygen (DO) was determined using a DO meter (HQ40d, HACH, Italy). Oxidation-reduction potential (ORP) was determined using an ORP meter (PRB100, HEEYIIS, China). Total nitrogen (TN), ammonia nitrogen (NH_4^+-N) and chemical oxygen demand

Table 1. Variation ranges of pH, DO, and ORP in CW effluents under different SER (statistical significance of differences among data sets was assigned at $p<0.05$).

Reactor	SER	Sampling port	Range of pH	Range of DO ($mg.L^{-1}$)	Range of ORP (mV)
CW0	2:1	A	7.59-7.69	3.59-3.78	203.0-239.0
		B	7.83-7.85	2.59-3.00	185.0-243.0
	1:2	A	7.44-7.72	3.96-4.22	251.0-285.0
		B	7.91-7.92	2.42-3.29	198.0-252.0
CW1	2:1	A	9.06-9.18	2.65-2.70	3.0-159.0
		B	8.43-9.31	1.80-2.38	97.0-203.0
	1:2	A	9.51-9.74	2.75-2.94	-74.0-169.0
		B	8.13-9.69	1.78-2.45	125.0-183.0
CW2	2:1	A	7.94-8.14	3.33-3.37	140.0-226.0
		B	9.52-9.53	1.17-2.03	77.0-124.0
	1:2	A	7.62-7.79	3.68-3.93	135.0-162.0
		B	9.09-9.13	1.68-2.76	-123.0-99.0

(COD) were analyzed immediately using a multi-parameter colorimeter (DR3900, HACH, USA). Nitrate (NO_3^--N) was analyzed with an ultraviolet and visible spectrophotometer according to the standard method. Three replicates were conducted for each sample and statistical analyses were performed and visualized with Origin 8.0 software. The differences among data sets were determined by the ANOVA with the significant at $p<0.05$.

Results and Discussion

Profiles of pH, DO and ORP in experimental CWs under different SER are shown in Fig. 2. Table 1 presents the variation ranges of pH, DO and ORP in CW effluents under different SER. As demonstrated by Table 1 and Fig. 2, the pH range in CW0-A and CW2-A was lower than that in CW0-B and CW2-B. The aerobic condition in the upper area of wetland was beneficial for nitrification that would consume a certain alkalinity. On the other hand, the pH range in CW1-A was higher than that in CW1-B which was ascribed to the reaction that $O_2+2H_2O+4e^-\rightarrow 4OH^-$ by micro-electrolysis occurring in upper nitrification area with Fe-C filler [15]. Effluent DO content in upper area of all experimental systems was significantly higher than that in bottom area. This phenomenon could be explained by two facts: (1) atmospheric reaeration and plants' oxygen transition in upper area of wetland system enhanced oxygen level [16]; (2) upper nitrification area was operated by tidal flow mode which promoted oxygen penetrating into wetland and improved overall oxygen environment. When SER was 2:1, the DO range in CW1-A (2.65-2.70 mg.L^{-1}) was inferior to CW0-A (3.59-3.78 mg.L^{-1}) and CW2-A (3.33-3.37 mg.L^{-1}). The decrease of DO in CW1-A was ascribed to iron oxidation and corrosion resulting from micro-electrolysis structure. Effluent DO concentration in all experimental systems under SER of 2:1 was lower than that under SER of 1:2. The results indicated that the extension of emptying status under tidal flow operation mode could promote

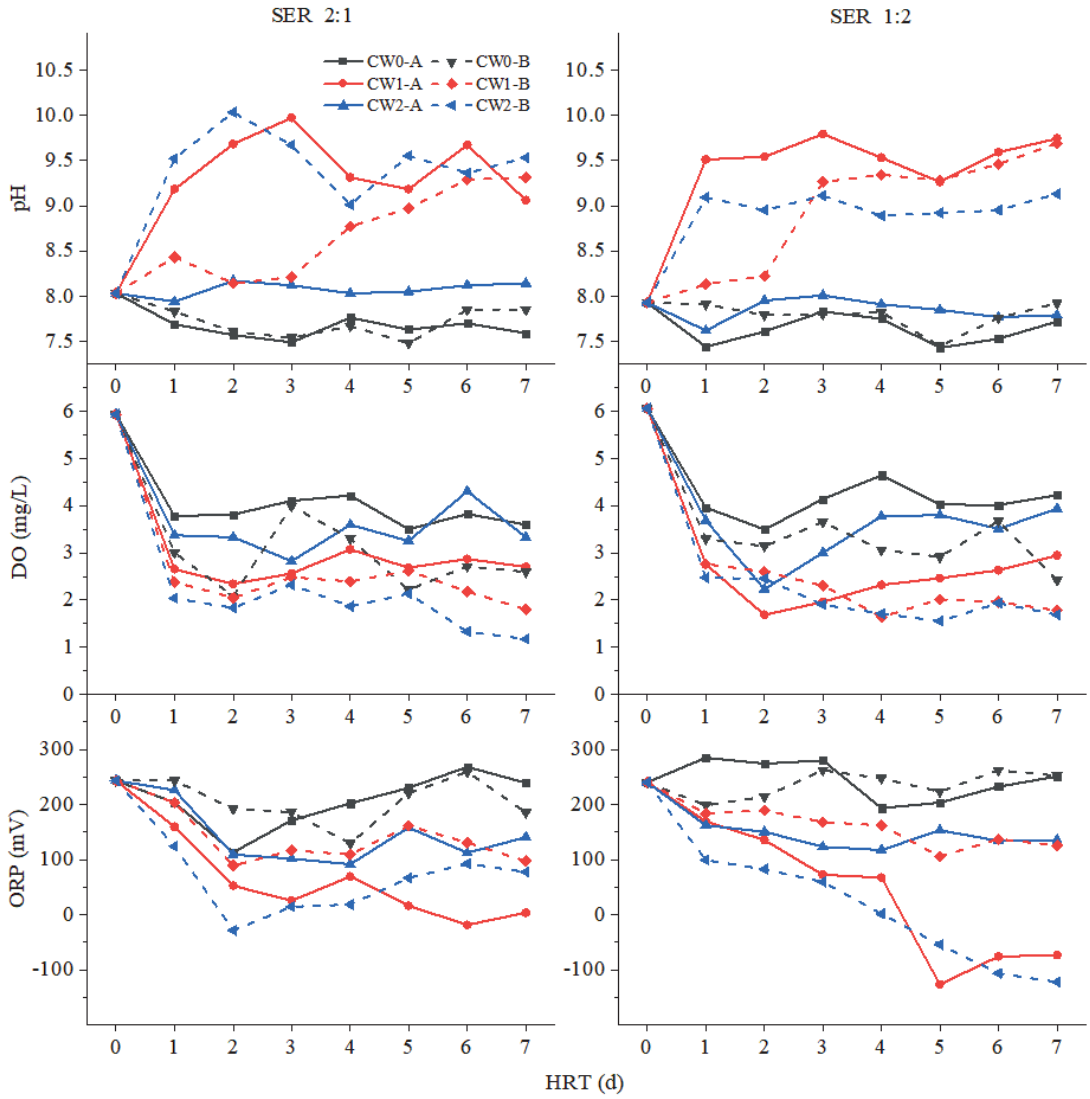

Fig. 2. Profiles of pH, DO and ORP in experimental CWs under different SER.

Table 2. Pollutant removal performance in CWs under different SER (statistical significance of differences among data sets was assigned at $p<0.05$).

Parameter	Influent ($mg.L^{-1}$)	SER	Sampling port	Effluent ($mg.L^{-1}$)	Removal (%)
NH_4^+-N	20.5±0.3	2:1	CW0-A	12.1±0.2	41.0±2.0
			CW1-A	12.9±0.2	37.1±2.0
			CW2-A	13.8±0.2	32.7±2.0
			CW0-B	13.1±0.2	36.1±2.0
			CW1-B	14.1±0.2	31.2±2.0
			CW2-B	16.8±0.2	18.0±2.0
		1:2	CW0-A	10.6±0.2	48.3±2.0
			CW1-A	12.1±0.2	41.0±2.0
			CW2-A	11.0±0.2	46.3±2.0
			CW0-B	11.2±0.2	45.4±2.0
			CW1-B	12.9±0.2	37.1±2.0
			CW2-B	13.4±0.2	34.6±2.0
NO_3^--N	14.5±0.3	2:1	CW0-A	7.3±0.2	49.7±2.0
			CW1-A	5.5±0.2	62.1±2.0
			CW2-A	4.0±0.2	72.4±2.0
			CW0-B	4.8±0.2	66.9±2.0
			CW1-B	3.2±0.2	77.9±2.0
			CW2-B	2.9±0.2	80.0±2.0
		1:2	CW0-A	6.0±0.2	58.6±2.0
			CW1-A	3.8±0.2	73.8±2.0
			CW2-A	3.2±0.2	77.9±2.0
			CW0-B	5.5±0.2	62.1±2.0
			CW1-B	3.2±0.2	77.9±2.0
			CW2-B	2.6±0.2	82.1±2.0
TN	36.5±0.5	2:1	CW0-A	19.7±0.3	46.0±2.0
			CW1-A	18.6±0.3	49.0±2.0
			CW2-A	18.1±0.3	50.4±2.0
			CW0-B	18.2±0.3	50.1±2.0
			CW1-B	17.7±0.3	51.5±2.0
			CW2-B	19.9±0.3	45.5±2.0
		1:2	CW0-A	16.8±0.3	54.0±2.0
			CW1-A	16.2±0.3	55.6±2.0
			CW2-A	14.4±0.3	60.5±2.0
			CW0-B	17.0±0.3	53.4±2.0
			CW1-B	16.5±0.3	54.8±2.0
			CW2-B	16.2±0.3	55.6±2.0

Table 2. Continued.

COD	120.0±3.0	2:1	CW0-A	47.0±2.0	60.8±2.0
			CW1-A	34.0±2.0	71.7±2.0
			CW2-A	31.0±2.0	74.2±2.0
			CW0-B	36.0±2.0	70.0±2.0
			CW1-B	32.0±2.0	73.3±2.0
			CW2-B	30.0±2.0	75.0±2.0
		1:2	CW0-A	40.0±2.0	66.7±2.0
			CW1-A	38.0±2.0	68.3±2.0
			CW2-A	25.0±2.0	79.2±2.0
			CW0-B	38.0±2.0	68.3±2.0
			CW1-B	22.0±2.0	81.7±2.0
			CW2-B	19.0±2.0	84.2±2.0

oxygen infiltration and enhance oxygen content. Redox potential generally decreases from surface to deep area and the upper area tend to have a higher redox because of oxygen diffusion [17]. ORP profiles were correlated with the variation of DO. Under SER of 1:2, the ORP value in CW1-A were in the ranges of 3.0 mV to 159.0 mV, which was lower than that in CW1-B ranging from 97.0 mV to 203.0 mV. Correspondingly, the ORP value in CW2-B were in the ranges of -123.0 mV to 99.0 mV, which was lower than that in CW2-A ranging from 135.0 mV to 162.0 mV. The presence of Fe-C micro-electrolysis structure facilitated the iron oxide reduction reactions thus the trend of reducibility was observed in iron-carbon zone of CWs.

Pollutant removal performance in CWs under different SER was shown in Table 2. COD removal was relatively higher in the bottom area of CWs under different SER than that in the upper area. 70.0±2.0%, 73.3±2.0% and 75.0±2.0% of COD were removed in CW0-B, CW1-B and CW2-B when SER was 2:1. Higher removal performance was obtained in CW1-B and CW2-B due to macro-molecular organics degraded into micro-molecular organics by Fe-C micro-electrolysis reaction, which was preferably utilized by heterotrophic denitrification. COD removal was 81.7% and 84.2 % in CW1-B and CW2-B under SER of 1:2, which were significantly higher than that in CWs under SER of 2:1 ($p < 0.05$). The main reason included: (1) COD removal was consistent with the variation of DO content and the good oxygen condition under SER of 1:2 could increase the degradation rate of organic matter [18]; (2) the long drained time was beneficial for mutual reaction between heterotrophic microbes and organic matter [19]. In view of the insufficiency in residual organic matter for heterotrophic denitrification, autotrophic denitrification could be driven by the iron oxidation and transfer that providing electron donor for the synergistic enhancement of subsequent denitrification.

Fig. 3 depicted the profiles of NH_4^+-N and NO_3^--N in experimental CWs under different SER. On the whole, NH_4^+-N removal in experimental CWs under different SER showed a downward trend with HRT. NH_4^+-N reductions were greater in the upper area of CWs under different SER than those in the bottom area, where the aerobic condition was favorable for the occurrence of nitrification reaction [20]. Simultaneously, 48.3±2.0%, 41.0±2.0% and 46.3±2.0% of NH_4^+-N were removed in CW0-A, CW1-A and CW2-A when SER was 1:2. There was no significant difference in NH_4^+-N removal between CW0-A and CW2-A, whereas NH_4^+-N removal in CW0-A and CW2-A was higher than that in CW1-A. The main reason was that oxygen exhausted by iron oxidation of micro-electrolysis reaction occurring in upper nitrification area of CW1 was unfavorable for the transformation of NH_4^+-N by nitrification. In contrast, 41.0±2.0%, 37.1±2.0% and 32.7±2.0% of NH_4^+-N were removed in CW0-A, CW1-A and CW2-A when SER was 2:1. The increase in emptying time of CWs provided a longer contact time between air and the pore spaces of substrate, strengthened the reoxygenation of substrates and further benefited nitrification process.

NO_3^--N reductions were uniformly greater in the bottom area of CWs under different SER than those in the upper area, where the anoxic condition promoted denitrification. Under SER of 2:1, 66.9±2.0%, 77.9±2.0% and 80.0±2.0% of NO_3^--N were removed in CW0-B, CW1-B and CW2-B. CW2-B exhibited the higher NO_3^--N removal than CW1-B while NO_3^--N removal in CW1-B and CW2-B was significantly higher than that in CW0-B ($p < 0.05$). The phenomenon could be explained by the fact that iron electrolysis generated different valence states that facilitating electron transport, thus enhancing denitrification performance [21]. Bottom denitrification area of CW2 was packed with Fe-C filler, thus further facilitated the occurrence of denitrification. In contrast, 62.1±2.0%, 77.9±2.0% and 82.1±2.0% of NO_3^--N were removed in CW0-B, CW1-B and CW2-B when SER was 1:2. However, no statistical difference in NO_3^--N removal of experimental CWs under different SER, which indicated that SER did not impart a significant impact on NO_3^--N removal. TN

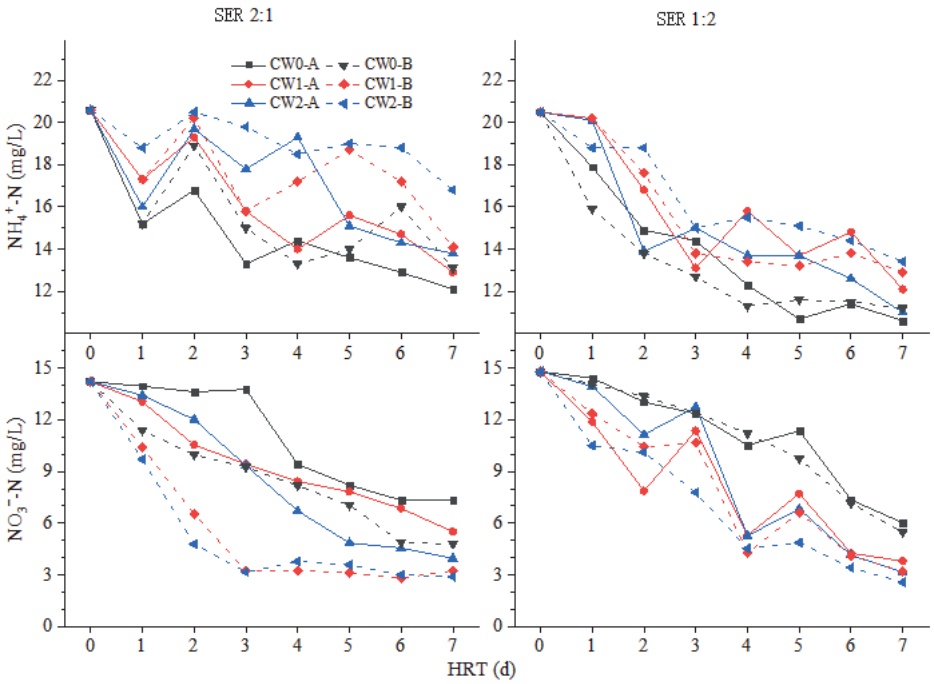

Fig. 3. Profiles of NH_4^+-N and NO_3^--N in experimental CWs under different SER.

was mainly composed of NH_4^+-N and NO_3^--N, hence favorable carbon and oxygen level contributed to the synergistic occurrence of nitrification and denitrification for efficient TN removal [22]. Submerged emptying ratio and the presence of iron-carbon filler imparted a certain influence on TN removal ($p < 0.05$), but there was no statistical difference on TN removal between upper nitrification area and bottom denitrification area of CWs. Under SER of 2:1, 50.1±2.0%, 51.5±2.0% and 45.5±2.0% of TN were removed in CW0-B, CW1-B and CW2-B. In contrast, 53.4±2.0%, 54.8±2.0% and 55.6±2.0% of TN were removed in CW0-B, CW1-B and CW2-B when SER was 1:2. A slight increase in TN removal of bottom denitrification area occurred between SER of 2:1 and 1:2, which exhibited similar variation with NO_3^--N removal. It made clear that nitrification in upper area contributed to nitrogen transformation (NH_4^+-N to NO_3^--N) while denitrification in bottom area contributed to NO_3^--N removal from water body thus facilitating TN removal [23].

Conclusions

The capacity of nitrification and denitrification was limited under carbon and oxygen deficiency condition. Partial tide flow operation mode in CWs created aerobic-anoxic alternative environment for the simultaneous occurrence of nitrification and denitrification. Effective transformation of NH_4^+-N to NO_3^--N mainly occurred in the upper area that is under tidal flow operation with a more oxidized condition. Extension of emptying status promoted better oxygen input for facilitating NH_4^+-N removal efficiencies. NO_3^--N reductions were uniformly greater in the bottom area of CWs. Better NO_3^--N removal performance was obtained in CWs via micro-electrolysis and autotrophic denitrification which was driven by the iron oxidation and transfer that providing electron donor for the synergistic enhancement of denitrification. Complete TN removal profited from efficient nitrification and denitrification. The study may provide an energy-saving and efficient solution to enhance nitrogen removal of eutrophic water.

Acknowledgment

This study was supported by the National Natural Science Foundation of China (grant No. 51809162) and National Key Research and Development Project (grant No. 2019YFC0408604).

Conflict of Interest

The authors have not declared any conflict of interest.

References

1. LI J., FAN J.L., ZHANG J., HU Z., LIANG S. Preparation and evaluation of wetland plant-based biochar for nitrogen removal enhancement in surface flow constructed wetlands. Environmental Science and Pollution Research, **25**, 13929, **2018**.

2. CUI X.J., ZHANG M.P., DING Y.J., SUN S.S., HE S.B., YAN P. Enhanced nitrogen removal via iron-carbon micro-electrolysis in surface flow constructed wetlands: Selecting activated carbon or biochar? Science of The Total Environment, **815**, 152800, **2022**.
3. WANG W., SONG X.S., LI F.Y., JI X.Y., HOU M.F. Intensified nitrogen removal in constructed wetlands by novel spray aeration system and different influent COD/N ratios. Bioresource Technology, **306**, 123008, **2020**.
4. CHEN Y.R., ZHANG J., GUO Z.Z., LI M., WU H.M. Optimizing agricultural biomass application to enhance nitrogen removal in vertical flow constructed wetlands for treating low-carbon wastewater. Environmental Research, **209**, 112867, **2022**.
5. HUA G.F., LI J.L., CHENG Y., KONG J., LIU X.D., SHI Y., HUANG Y.Y. Efficiencies of nitrogen removal in slope-constructed wetlands. Polish Journal of Environmental Studies, **30** (3), 2107, **2021**.
6. MA Y.H., ZHENG X.Y., HE S.B., ZHAO M. Nitrification, denitrification and anammox process coupled to iron redox in wetlands for domestic wastewater treatment. Journal of Cleaner Production, **300**, 126953, **2021**.
7. DING Y., SUN Y., FENG D.L., LIU X.P., SONG X.S. Synergistic effects of high rate algal pond and submerged macrophyte pond on constructed wetland for water purification. Polish Journal of Environmental Studies, **30** (5), 4887, **2021**.
8. DING Y., LIN G.W., LIU X.P., SONG X.S. Enhanced nitrogen removal of eutrophic water in constructed wetland by novel integration of submerged macrophyte pond. Polish Journal of Environmental Studies, **31** (3), 2485, **2022**.
9. LIU J., GAO F., GAO M.C., ZHAO Y.G., GUO L., JIN C.J., JI J.Y., SHE Z.L. Effects of flow mode on the performance and microbial community in tidal flow constructed wetland treating mariculture wastewater. Journal of Water Process Engineering, **47**, 102850, **2022**.
10. ZHAO L., FU G.P., PANG W.C., TANG J., GUO Z.P., HU Z.L. Biochar immobilized bacteria enhances nitrogen removal capability of tidal flow constructed wetlands. Science of The Total Environment, **836**, 155728, **2022**.
11. XU D., LIN L.L., XU P., ZHOU Y., XIAO E.R., HE F., WU Z.B. Effect of drained-flooded time ratio on ammonia nitrogen removal in a constructed wetland-microbial fuel cell system by tidal flow operation. Journal of Water Process Engineering, **44**, 102450, **2021**.
12. JU X.X., WU S.B., ZHANG Y.S., DONG R.J. Intensified nitrogen and phosphorus removal in a novel electrolysis-integrated tidal flow constructed wetland system. Water Research, **59**, 37, **2014**.
13. ZHENG X.Y., JIN M.Q., ZHOU X., CHEN W., LU D., ZHANG Y., SHAO X.Y. Enhanced removal mechanism of iron carbon micro-electrolysis constructed wetland on C, N, and P in salty permitted effluent of wastewater treatment plant. Science of The Total Environment, **649**, 21, **2019**.
14. MA X.N., LI X., LI J., REN J.L., CHI L., CHENG X.W. Iron-carbon could enhance nitrogen removal in *Sesuvium portulacastrum* constructed wetlands for treating mariculture effluents. Bioresource Technology, **325**, 124602, **2021**.
15. DENG S.H., LI D.S., YANG X., CAI Q.Q., PENG S., PENG X.N., YAO H., XIE B.H. Novel characteristics on micro-electrolysis mediated Fe(0)-oxidizing autotrophic denitrification with aeration: Efficiency, iron-compounds transformation, N_2O and NO_2^- accumulation, and microbial characteristics. Chemical Engineering Journal, **387**, 123409, **2020**.
16. ZHANG X.Y., LI X., HAN Q.J., JU K., WEI D.Y., SUN Y.Q., WAN Q. Effects of hydraulic retention time (HRT) and packing height on the performance of homemade ceramsite-soil constructed wetland for rural domestic wastewater treatment. Polish Journal of Environmental Studies, **30** (5), 4845, **2021**.
17. ROTH J.J., PASSIG F.H., ZANETTI F.L., PELISSARI C., SEZERINO P.H., NAGALLI A., CARVALHO K.Q.D. Influence of the flooded time on the performance of a tidal flow constructed wetland treating urban stream water. Science of The Total Environment, **758**, 143652, **2021**.
18. JIA W.L., ZHANG J., WU J., XIE H.J., ZHANG B. Effect of intermittent operation on contaminant removal and plant growth in vertical flow constructed wetlands: A microcosm experiment. Desalination, **262**, 202, **2010**.
19. PANG Q.Q., XU W.W., HE F., PENG F.Q., ZHU X., XU B., YU J.H., JIANG Z.W., WANG L.M. Functional genera for efficient nitrogen removal under low C/N ratio influent at low temperatures in a two-stage tidal flow constructed wetland. Science of The Total Environment, **804**, 150142, **2022**.
20. WANG W., DING Y., ULLMAN J.L., AMBROSE R.F., WANG Y.H., SONG X.S., ZHAO Z.M. Nitrogen removal performance in planted and unplanted horizontal subsurface flow constructed wetlands treating different influent COD/N ratios. Environmental Science and Pollution Research, **23**, 9012, **2016**.
21. ZHAO Z.M., SONG X.S., ZHAO Y.F., XIAO Y.P., WANG Y.H., WANG J.F., YAN D.H. Effects of iron and calcium carbonate on the variation and cycling of carbon source in integrated wastewater treatments. Bioresource Technology, **225**, 262, **2017**.
22. CHAND N., KUMAR K., SUTHAR S. Enhanced wastewater nutrients removal in vertical subsurface flow constructed wetland: Effect of biochar addition and tidal flow operation. Chemosphere, **286**, 131742, **2022**.
23. LIU S.Y., YAN B.X., WANG L.X. The layer effect in nutrient removal by two indigenous plant species in horizontal flow constructed wetlands. Ecological Engineering, **37** (12), 2101, **2011**.